journal

J. Am. Ceram. Soc., 84 [7] 1627–31 (2001)

Role of Structural Fe(III) and Iron Oxide Nanophases in Mullite Coloration

Amédée Djemai,† Georges Calas,*,† and Jean Pierre Muller†,‡

Laboratoire de Minéralogie-Cristallographie, UMR 7590, CNRS, Universités Paris 6 et 7, IPGP, 75252 Paris, France

Institut de Recherche pour le Développement, 75480 Paris, France

Six mullite samples, derived from heat-treated natural kaolinites with various iron content, were investigated and compared to synthetic monophasic mullite. They were analyzed by X-ray diffraction, diffuse reflectance spectroscopy, and electron paramagnetic resonance. To quantify mullite coloration, the CIE colorimetric system was used. In contrast to synthetic mullite, samples showed charge transfer bands involving O^{2-} and Fe^{3+} ions as well as ferric crystal-field transitions due to Fe^{3+} ions in iron oxide nanoparticles. Absorption edges showed red shifts. The resulting yellowness, saturation of which increased with the content of iron oxide nanoparticles, is direct evidence for the coloring effect of Fe^{3+} ions.

I. Introduction

MULLITE is an important nonstoichiometric aluminosilicate material,[1] able to incorporate considerable amounts of impurities.[2–5] In particular, Fe^{3+} ions are mainly incorporated into the (AlO_6) octahedra, substituting for Al^{3+}.[2,4,5] Previous spectroscopic studies[6] have been carried out on Cr-doped mullite, but iron effects on ultraviolet (UV)–visible (vis) absorption spectra of mullite are poorly understood.[7]

Because many kaolinites used as ceramic raw materials contain iron as a common impurity, some of which ends up in the mullite phase after firing, it is important that the effect of iron be fully understood when deducing optical property information from UV–vis absorption spectra of mullite. Low UV transmittance in mullite has been reported[8] but has not been studied. For this reason, detailed information is required about the way in which the iron substitution and iron oxide impurities influence the spectral behavior of mullite. Diffuse reflectance spectroscopy (DRS) is the most appropriate technique for providing this information, but no such study has previously been reported. Previous spectroscopic studies have been carried out on the color changes of heated kaolinites[7,9,10] and ceramics.[11] However, they have shown the influence of only the bulk chemical content of iron and titanium impurities, but no relationship has been established between iron species, their distribution, and chromatic properties in mullite. Furthermore, spectral properties of superparamagnetic (nanocrystalline) ferric oxides are not known in mullite. Understanding the relationship between dilute Fe^{3+} ions, incorporated iron oxide nanophases, and optical parameters could help to manage the chromatic behavior in mullite ceramics. We present here new DRS studies of mullite, exhibiting yellow color which we attribute to Fe(III) ions.

R. A. Condrate—contributing editor

Manuscript No. 188722. Received February 23, 2000; approved March 9, 2000.
*Member, American Ceramic Society.
†Universités Paris 6 et 7.
‡Institut de Recherche pour le Developpement.

II. Experimental Procedure

Six mullite samples were investigated. They were formed from kaolinites (Table I), heated for 3 h at 1300°C in an electrically heated furnace, working under air atmosphere. The temperature was set by a Pt/Pt-Rh thermocouple inserted into the specimen ($\Delta T \approx \pm 2$°C). The heating rate used to reach the set temperature was 5°C/min. They were cooled down at 5°C/min in air.

The mullite powders were checked by scanning electronic microscopy (SEM) and then were characterized by X-ray diffraction (XRD) using a diffractometer (Model D500, Siemens, Karlsruhe, Germany) fitted with a vertical goniometer and Cu$K\alpha$ radiation selected by a graphite monochromator. The goniometer was set to scan from 10° to 70° 2θ at a speed of 0.04° per 20 s.

Samples with various iron contents were subsequently analyzed by DRS and electron paramagnetic resonance (EPR). DRS spectra were obtained between 220 and 800 nm at room temperature with a spectrophotometer (Model Cary 500, Varian, Victoria, Australia), equiped with a 10 cm diameter integrating sphere coated with Halon. EPR spectra were recorded at 140 K, in the 0 to 400 mT magnetic field range for X-band frequency ($\nu = 9.42$ GHz) using an EPR spectrometer (Model ESP 300E, Bruker Spectrospin SA, Wissembourg, France).

To quantify the color and to study its variation with the iron species content in mullite, we have choosen to use the CIE colorimetric system.[14,15] Optical properties in mullite were quantified, using chromaticity as well as Helmholtz coordinates, i.e., (i) the dominant wavelength (λ_D) related to the tint of the color and very sensitive to pigment content, (ii) the excitation purity (P_e) scaled between 0% for a colorless object and 100% for a pure color, and (iii) the luminance (%Y). Thus, λ_D, P_e, and %Y were derived from the optical spectra according to the 1931 standard observer of the CIE.[15] The three parameters are related to the hue, the saturation, and the reflectance, respectively.

III. Results and Discussion

(1) Mullite Characterization

Heat treatment produced mullite as the major crystalline compound. SEM characterization revealed the occurence of mullite crystals 100 to 200 nm in length and 25 to 50 nm in width. The principal impurities (Table I) in the studied mullite were iron and titanium.

(A) Aluminosilicate Matrix: Kaolinite–mullite transformations were similar for all starting materials, and the presence of crystalline mullite was evidenced by XRD. However, the Hor sample did not exhibit cristobalite reflections. XRD patterns showed, in addition to strong mullite reflections, cristobalite 101 and 200 reflections which appeared at 21.98° and 36° 2θ, and a weak broad background characteristic of an amorphous material extending from about 16° to 36° 2θ.

(B) Foreign oxides: Furthermore, anatase 101 and rutile 110 reflections were present with clearly resolved weak peaks which were observed, respectively, at 25.25° and 27.40° 2θ. Studied samples have exhibited superparamagnetic behavior,[5,10] assigned

Table I. Starting Kaolinite Characteristics*

Names‡	Phases§	Impurity content (wt%) Fe_2O_3	TiO_2	K_2O	Na_2O	Structural order HI¶	$E^{140K} \times 10^{2}$††
(1) A-88	An	1.72	1.09	<0.01	<0.01	0.30	15
(2) A-90	An	1.68	0.98	<0.01	<0.01	0.30	12
(3) Car	Qz, il, He	2.28	0.21	0.58	<0.01	~1.0	7
(4) KGa-2	An	1.13	2.08	0.07	<0.01	0.21	15
(5) Hor	Qz, il	0.88	0.07	1.5	<0.01	~1.0	6
(6) KGa-1	An	0.21	1.39	0.05	0.01	1.07	6

*Reference sample: synthetic monophasic mullite (wt%: Fe_2O_3 = 0.21; TiO_2 = 0.14), supplied by KPCL (Limoges, France). ‡Sources: (1, 2) Jari River (Amazon basin, Brazil); (3, 5) Carrara and Horri, respectively, from Embu and Jundiapeba areas (Sao Paolo, Brazil); (4, 6) Warren County (Georgia, USA). §From the XRD patterns the symbols are listed in the apparent order of importance of foreign phases identified: (An) anatase, (Qz) quartz, (il) illite, (He) hematite. ¶XRD index after Hinkley. ††E = EPR index measured at 140 K, where $E = L/D$; $D = B(3Z) - B(1Y)$ and L = line width at half-height, calculated on X-band.[1-6] Samples have been extensively described elsewhere.[12,13]

to iron-rich domains, but have not given in X-ray diffraction patterns. Therefore, the X-ray results imply crystalline particles too small to coherently scatter X-rays.[16] Consequently, by analogy with nanocrystalline hematite-bearing samples which have been extensively studied by Mössbauer spectroscopy,[16,17] it is inferred that the studied mullites incorporated iron oxide particles in the nanometric size range.

(2) Evidence for Structural Fe^{3+}

(A) Paramagnetic Species: All samples show most of the resonances that have been described for mullites. The X-band spectra are characterized by a complex EPR signal (see Fig. 1(a)) at low magnetic field (g_{eff} = 4.23; B = 160 mT), due to isolated Fe^{3+} ions at two tetrahedral (T) and octahedral (O) sites[2-5] in mullite. EPR studies[2-5] have established that iron, as Fe^{3+} substitutes for Al mainly in the octahedral sites, chains of which extend along the c-axis of the structure. The intensities of EPR signals at g_{eff} = 9 and g_{eff} = 4, corresponding, respectively, to octahedral and tetrahedral iron,[2,5] by analogy with an EPR study on Fe^{3+} center in sillimanite[18] which has a structure similar to that of mullite, were used to monitor Fe^{3+} content in the investigated samples. Figure 1(a) shows the EPR sensitivity to Fe(III) content which increases from reference to A-88 mullite.

(B) $O^{2-} \rightarrow Fe^{3+}$ Charge Transfer (OMCT): All optical spectra (see Fig. 2(a)) exhibit one strong charge transfer absorption band in the UV region. It may be assigned to charge transfer transitions between oxygen and Fe(III) cations.[19,20] At least one distinct charge transfer, peak can be observed at 253 nm (4.90 eV). This position seems to correspond to the ($6t_{1u} \rightarrow 2t_{2g}$) transition,[19,20] the energy of which was calculated to be at 262 nm (4.72 eV) in an octahedral FeO_6 cluster.[20] This assignment seems plausible because it has been shown that iron associated with mullite occurs chiefly as Fe^{3+} isomorphous substitution for Al^{3+} in octahedral coordination in the mullite lattice, as evidenced by EPR and Mössbauer results.[2,4,5,10] The increasing iron absorption (see Fig. 2(a)) from reference to A-88 mullite produces an edge shift extending to longer wavelength. The increasing intensity trend of the OMCT with structural Fe(III) content is quite similar to those obtained with EPR spectra. The intensities of the EPR signal at g_{eff} = 9 and OMCT (see Fig. 3) are strongly correlated, and consequently are assumed to arise from the same source, i.e., structural iron in octahedral coordination. It is inferred that increasing absorption in the UV range may be directly correlated with structural Fe(III) content. Referring to reflectance spectra

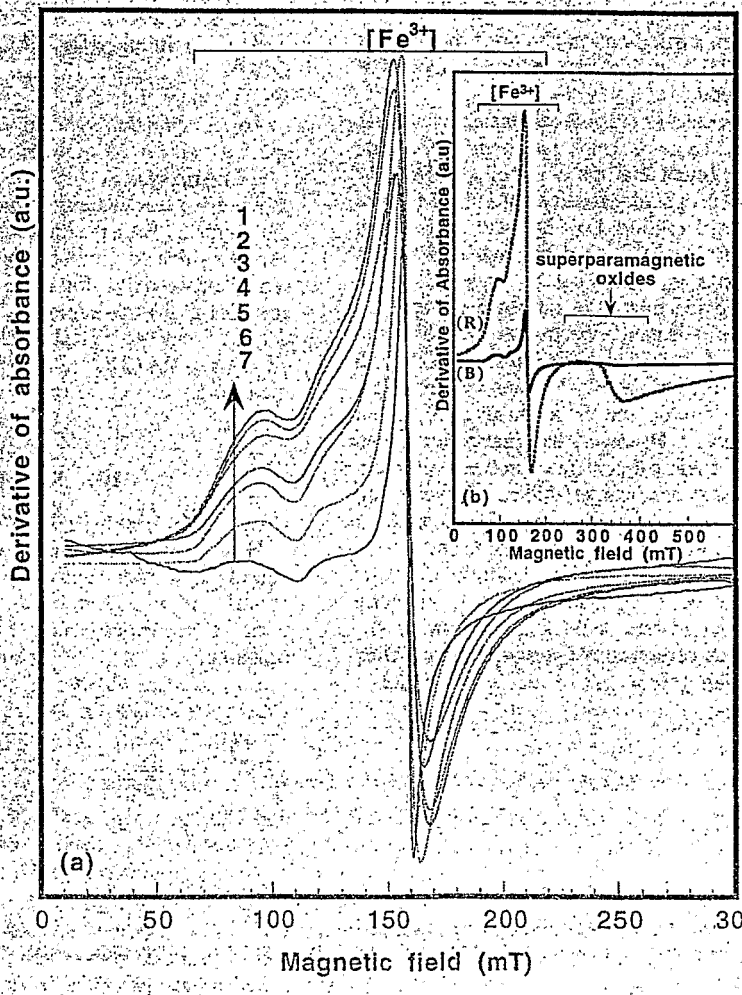

Fig. 1. X-band EPR spectra: (a) mullite: (1) A-88, (2) A-90; (3) Car, (4) KGa-2, (5) Hor; (6) KGa-1, and (7) ref. (synthetic sample); (b) Car mullite, derived from raw (R) and initially bleached (B) kaolinites.

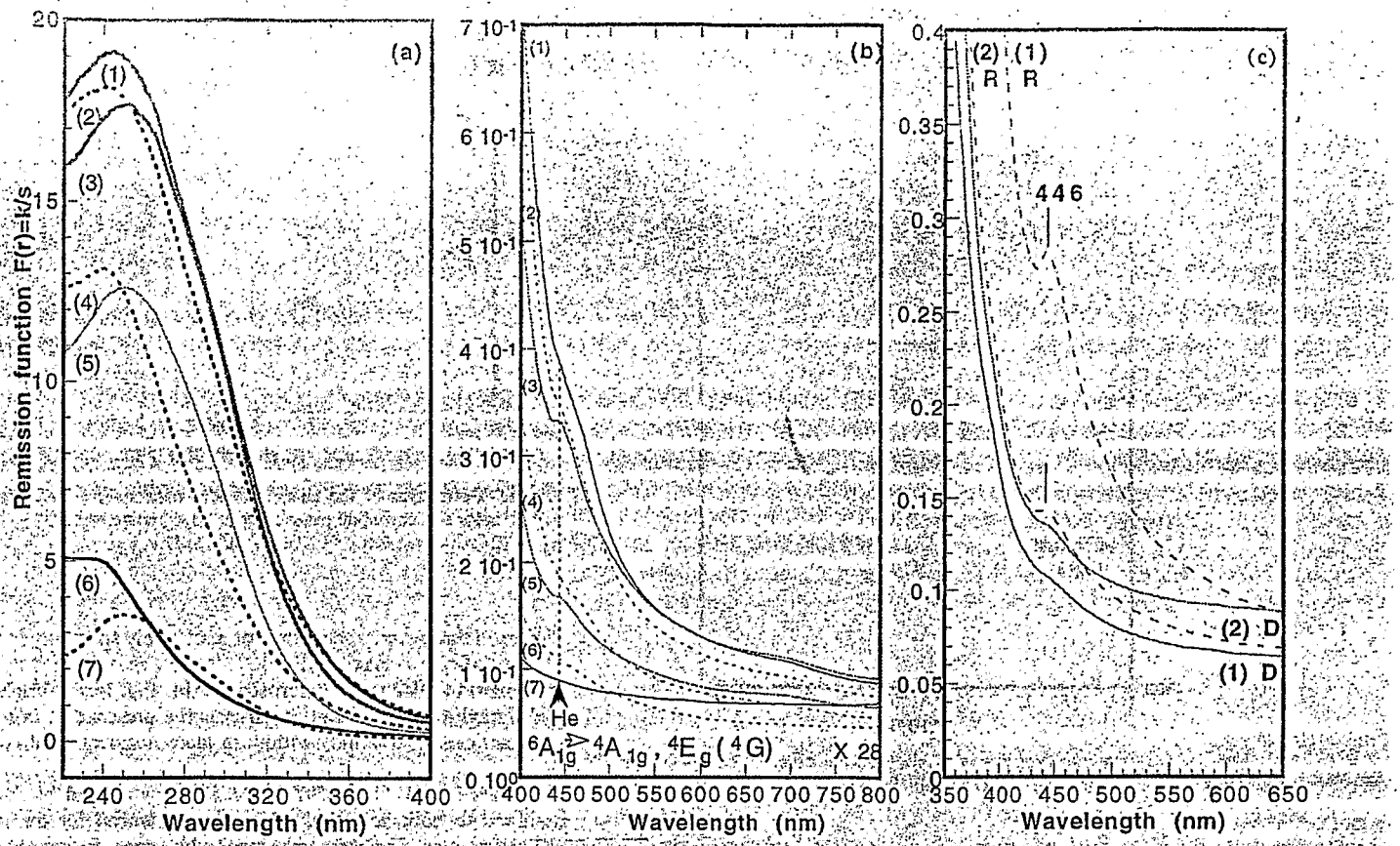

Fig. 2. Optical spectra of mullite: (1) A-88, (2) A-90, (3) Car, (4) KGa-2, (5) Hor, (6) KGa-1, and (7) synthetic sample; (a) $O^{2-} \rightarrow Fe^{3+}$ charge transfer band, (b) absorption edge shift and *d–d* transitions, (c) behavior of 446 nm transition in Car (1) and Hor (2) mullites, derived from raw (R) and deferrated (D) kaolinites.

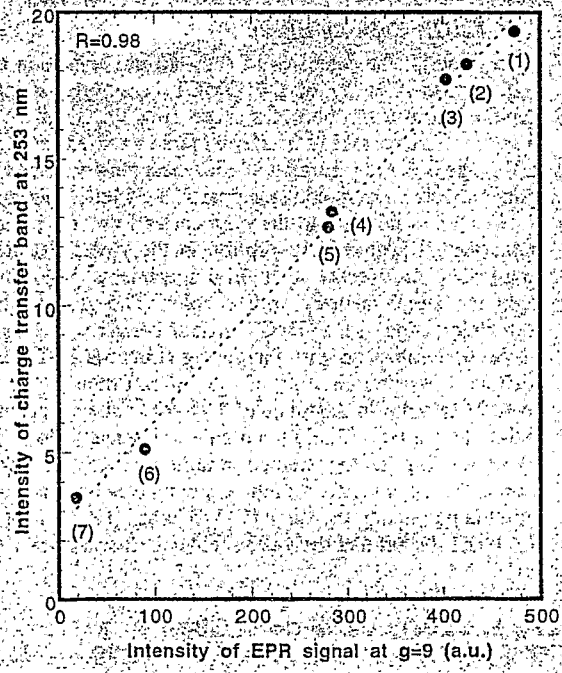

Fig. 3. Correlation of the EPR signal at $g = 9$ and charge transfer band of mullite: (1) A-88, (2) A-90, (3) Car, (4) KGa-2, (5) Hor, (6) KGa-1, and (7) reference (synthetic sample).

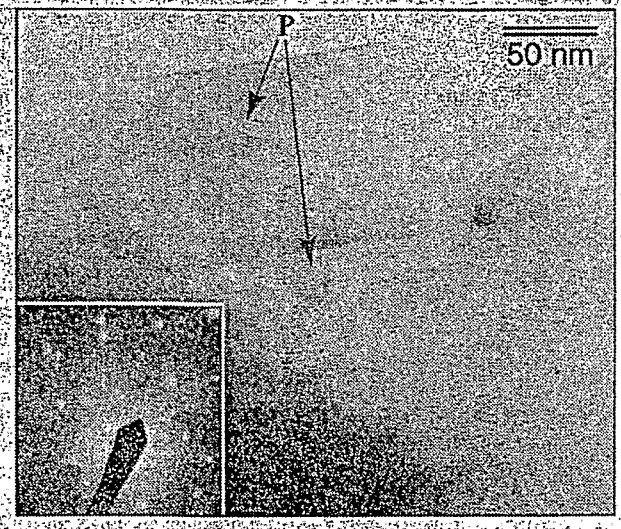

Fig. 4. Transmission electron micrograph of Car sample and corresponding selected area diffraction (SAD) pattern showing mullite reflections. P = iron oxide nanoparticles (5–7 nm).

from titaniferous varieties of andalousite, the charge transfer band in mullite has been attributed to $Fe^{2+} \rightarrow Fe^{3+}$, $Ti^{3+} \rightarrow Ti^{4+}$, and $Ti^{3+} + Fe^{3+} \rightarrow Ti^{4+} + Fe^{2+}$ transitions by earlier investigations.[7,11,21] The presence of ferrous iron seems unlikely because it is well known that the spin-allowed $^5T_2 \rightarrow {}^5E(D)$ transition for this ion in an octahedral site occurs at approximately 1000 nm.[22] The studied mullite spectra do not show it. Further, associated rutile occurs as an independent phase, according to the XRD data. Consequently, for such charge transfer to take place, it is considered necessary that most of the Ti^{4+} and Fe^{3+} ions substitute for octahedral Al^{3+} in the mullite structure. In agreement with the XRD data, the absorption threshold of rutile was observed at 388 nm.[23,24]

(3) Evidence for Iron Oxide Nanophases

In visible spectra, the spectral features due to the higher-energy intracationic *d–d* transitions are obscured by intense absorption

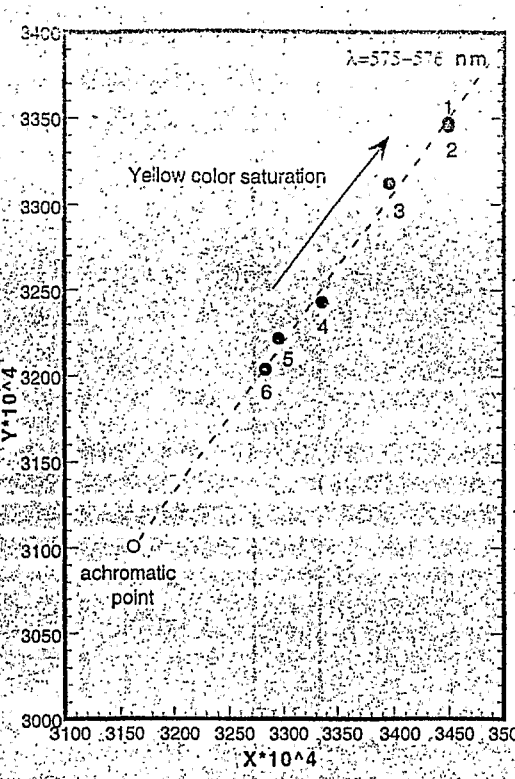

Fig. 5. Chromaticity coordinates (x,y) of mullite samples: (1) A-88, (2) A-90, (3) Car, (4) KGa 2, (5) Hor, and (6) KGa-1.

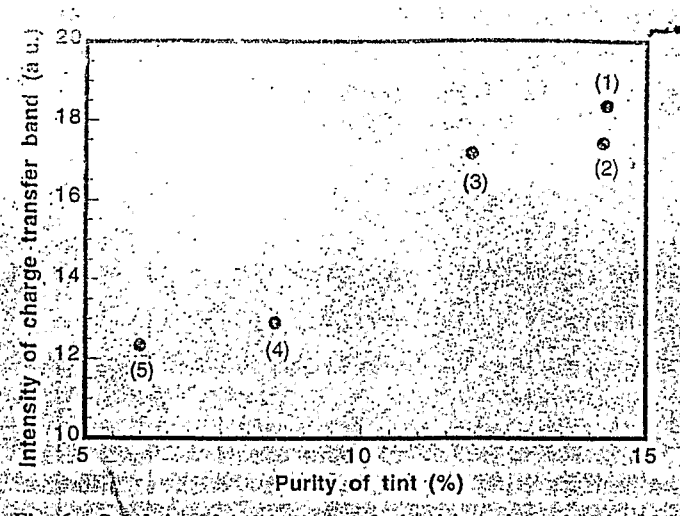

Fig. 6. Correlation of the charge transfer band intensity and purity of yellow color tint in mullite samples with Fe_2O_3 content (wt %) > 0.5: (1) A-88, (2) A-90; (3) Car, (4) KGa-2, and (5) Hor.

due to the $O^{2-} \rightarrow Fe^{3+}$ OMCT process. However, the spectra plotted in Fig. 2(b) show an absorption edge near 446 nm, which, because of its intensity and energy, can be ascribed, with a fair degree of certainty, to d–d transitions of octahedrally coordinated Fe^{3+}. The feature at 446 nm, which is particularly evident in the spectra of the A-88, A-90, Car, KGa-2, and Hor samples, is attributed to degenerated crystal-field-independent $^6A_{1g} \rightarrow {}^4A_{1g}$, ^4E_g (^4G) transitions of Fe^{3+} in iron oxide particles by analogy with spectral features of hematite nanophases dispersed through silica gel.[25] This assignment is supported for the following reasons: (i) the EPR signal at high magnetic field (see Fig. 1(b)) due to superparamagnetic iron oxides strongly decreases and in the same way is evidence for intense Fe(III) ion incorporation (increasing EPR signal at $g_{eff} = 9$ and $g_{eff} = 4.3$) in mullites derived from unbleached heated kaolinites; (ii) optical spectra do not exhibit an evident absorption edge near 446 nm in mullites derived from initially bleached kaolinite specimens (see Fig. 2(c)). It is inferred that the 446 nm feature is evidently due to d–d electronic transitions in Fe^{3+} of incorporated (residual) iron oxide nanoparticles as evidenced by EPR and Mössbauer data.[5,10] Notwithstanding that the intensity of the 446 nm feature is reached by the tail of the OMCT band, it seems reasonable to suggest that its sharpness may be related to increased iron oxide nanophase concentration.[25] Further, iron oxide nanophases evidenced by DRS and EPR data most likely occur in pigmentary form, that is, as particles, dispersed throughout the volume of a relatively spectrally invariant aluminosilicate matrix (mullite). This view is supported by using transmission electronic microscopy. In Fig. 4, a bright-field micrograph of the Car sample reveals the presence of iron oxide nanoparticles (≈5–7 nm) within an aluminosilicate matrix (mullite).

Consequently, the well-defined absorption band at 860 nm, assigned to bulk hematite,[17] was not evidenced for the studied mullite spectra. This is in agreement with earlier investigations on spectral properties of superparamagnetic hematite.[17] However, this band was observed in the optical spectra of the parental kaolinites, heated from 500° up to 900°C (manuscript in progress).

(4) *Fe(III) Coloring Effect*

In general, the intensity of the 446 nm transition (Fig. 2(b)) follows the intensity of the OMCT band. The shaped feature centered at 446 nm becomes more pronounced as the structural iron content increases. It is inferred that increased absorption in the UV range is directly correlated with the intensity of the ligand field transition due to iron oxide nanoparticle content. This suggests that the feature is inherent to the pigment and that the pigment is the same for all samples. Absorption in the violet and blue regions dominates the spectra of mullite specimens, giving transmitted light its complementary yellow color. The gradual shift of the absorption edge of the OMCT band to longer wavelength and the absorption enhanced with increasing structural Fe(III) content, as well as increasing intensity of the 446 nm transition from KGa-1 to A-99 samples in the range of 340–500 nm, are accompanied by a tint change (see Fig. 5) from pale to intense yellow. The points corresponding to the studied mullites lie on one straight line passing through the achromatic C point. This line indicates that λ_D (hue) is practically the same (575–576 nm) for all samples (Table II). It is inferred that the yellow color is characteristic of mullites

Table II. Chromatic and Helmholtz (λ_D, P_e, Y) Coordinates for Used Mullites

	Samples†					
	1	2	3	4	5	6
Coordinates						
x	0.3347	0.3345	0.3312	0.3243	0.3204	0.3222
y	0.3449	0.3449	0.3396	0.3336	0.3283	0.3295
Properties						
%Y	59.28	59.32	59.10	66.69	65.37	69.15
λ_D (nm)	575.0	575.4	576.2	574.9	575.4	576.2
P_e (%)	14.30	14.24	11.94	8.47	5.99	6.82

†(1) A-88, (2) A-90, (3) Car, (4) KGa-2, (5) Hor, (6) KGa-1.

obtained from fired raw kaolinites. The other main consequence is that the P_e of tint and the %Y (Table II) in mullite change with iron content. The most suitable representation of change in purity of tint in the different samples is obtained by plotting P_e against pigmenting iron species content. Two parameters can be considered from optical spectra: (i) the band position and (ii) the band intensity, which relate to the content of the coloring pigment. The intensity of the OMCT band (Fig. 6) is strongly correlated with the purity of tint in mullite. This is direct evidence for the role of Fe(III) in the specific mullite yellow coloration, saturation of which arises mainly from the increasing content of Fe(III). The luminance values (Table II) decrease sharply in the yellow region when the purity of tint is higher than 12% in A-88, A-90, and Car mullites. It might be related to an increased concentration of iron oxide nanophases.

IV. Conclusion

Mullite samples derived from heat-treated raw kaolinites exhibit charge transfer bands involving oxygen (O^{2-}) and iron (Fe^{3+}) ions as well as ferric crystal-field transitions due to Fe^{3+} ions in iron oxide nanoparticle inclusions.

On the other hand, the KGa-1 sample and the synthetic monophasic mullite, both containing less than 0.22 wt% Fe_2O_3, do not show ferric crystal-field transitions. This probably means that all structural iron enters the Al^{3+} octahedral sites of mullite.

The occurrence of iron oxide particles in the nanosize range is confirmed by an EPR signal due to superparamagnetic oxides and supported by transmission electronic microscopy of mullite samples, derived from raw and initially bleached kaolinites.

With increasing structural iron and iron oxide nanoparticle contents, absorption edges of charge transfer bands show red shifts in the visible spectrum.

The resulting yellowness ($\lambda = 575$–576 nm) of mullites is direct evidence for the role of Fe^{3+} ions in the coloring effect, saturation of which arises mainly from the increasing content of Fe^{3+} ions in iron oxide particles on the nanosize scale. A Mie scattering process may occur in mullite samples, since the particle sizes are much smaller than the wavelength of the light.

As a consequence, the increasing whiteness of samples with a lack of iron inclusions might be explained by iron incorporation into the mullite structure.

It is well known[26] that the increasing iron solubility process is a temperature-controlled mechanism up to the solid solubility limit of iron in mullite.[26,27]

References

[1]W. E. Cameron, "Composition and Cell Dimensions of Mullite," *Am. Ceram. Soc. Bull.*, **56**, 1003–1007 (1977).

[2]H. Schneider and H. Rager, "Iron Incorporation in Mullite," *Ceram. Int.*, **12**, 117–25 (1986).

[3]H. Rager, H. Schneider, and H. Graetsch, "Chromium Incorporation in Mullite," *Am. Mineral.*, **75**, 392–97 (1990).

[4]C. M. Cardile, I. W. M. Brown, and K. J. D. Mackenzie, "Mössbauer [illegible] and Lattice Parameters of Iron-Substituted Mullites," *J. Mater. Sci. Lett.*, **6**, 357–62 (1987).

[5]A. Djemai, E. Balan, G. Morin, G. Hernandez, J. C. Labbe, and J. P. Muller, "Behavior of Paramagnetic Iron during Thermal Transformations of Kaolinite," *J. Am. Ceram. Soc.*, **84** [5] 1017–24 (2001).

[6]K. Ikeda, H. Schneider, M. Akasaka, and H. Rager, "Crystal-Field Spectroscopic Study of Cr-Doped Mullite," *Am. Mineral.*, **77**, 251–57 (1992).

[7]J. A. Homor, "The Effect of Calcination on the Diffuse Reflectance and Phase Transformations of Kaolinite"; Ph.D. Thesis, Rutgers University, New Brunswick, NJ, 1984.

[8]H. Schneider, M. Schmücker, K. Ikeda, and W. A. Kaysser, "Optical Translucent Mullite Ceramics," *J. Am. Ceram. Soc.*, **76** [11] 2912–14 (1993).

[9]P. Sennet, "Changes in the Physical Properties of Kaolin on Exposure to Elevated Temperature," *Sci. Geol. Mém.*, **89**, 71–79 (1990).

[10]E. Murad and U. Wagner, "Mössbauer Spectra of Kaolinite, Halloysite and the Firing Products of Kaolinite: New Results and a Reappraisal of Published Work," *Neues Jahrb. Mineral., Abh.*, **162** [3] 281–309 (1991).

[11]C. S. Hogg and F. R. Noble, "A Kubelka–Munk Analysis of the Influence of Iron and Titanium Oxides on the Optical Properties of Hard Porcelain," *Sci. Ceram.*, **10**, 703–10 (1979).

[12]H. H. Murray and P. Partridge, "Genesis of Rio Jari Kaolin," *Dev. Sedimentol.*, **35**, 279–91 (1982).

[13]H. H. Murray, "Kaolin Minerals, Their Genesis and Occurences"; pp. 67–89 in Reviews in Mineralogy, Vol. 19, *Hydrous Phyllosilicates*. Edited by S. W. Bailey. Mineralogical Society of America, Washington, D.C., 1988.

[14]G. Wyszecki and W. S. Stiles, *Color Science: Concepts and Methods, Quantitative Data and Formulae*, 2nd ed. Wiley, New York, 1982.

[15]A. Bedidi, B. Cervelle, J. Madeira, and M. Pouget, "Moisture Effects on Visible Spectral Characteristics of Lateritic Soils," *Soil Sci.*, **153**, 129–41 (1992).

[16]W. Kundig, H. Bommel, R. H. Linquist, G. Constabaris, and R. H. Linquist, "Some Properties of Supported Small α-Fe_2O_3 Particles Determined with the Mössbauer Effect," *Phys. Rev.*, **142**, 327–33 (1966).

[17]R. V. Morris, D. G. Agresti, H. V. Lauer, J. A. Newcomb, T. D. Sheler, and A. V. Murali, "Evidence for Pigmentary Hematite on Mars Based on Optical, Magnetic and Mössbauer Studies of Superparamagnetic (Nanocrystalline) Hematite," *J. Geophys. Res.*, **94** [B3] 2760–78 (1989).

[18]J. Le Marshall, D. R. Hutton, G. J. Troup, and J. R. W. Thyer, "A Paramagnetic Resonance Study of Cr^{3+} and Fe^{3+} in Sillimanite," *Phys. Status Solidi*, **A5**, 769–73 (1971).

[19]D. M. Sherman, "Electronic Spectra of Fe^{3+} Oxides and Oxide Hydroxides in the Near IR to Near UV," *Am. Mineral.*, **70**, 1262–69 (1985).

[20]D. M. Sherman, "Molecular Orbital (SCF-Xα-SW) Theory of Metal–Metal Charge Transfer Processes in Minerals. I. Applications to $Fe^{2+} \rightarrow Fe^{3+}$ Charge Transfer and 'Electron Delocalization' in Mixed-Valence Iron Oxides and Silicates. II. Applications to $Fe^{3+} \rightarrow Ti^{4+}$ Charge Transfer Transitions in Oxides and Silicates," *Phys. Chem. Miner.*, **14**, 355–67 (1987).

[21]W. E. Cameron, "Nonstoichiometry in Sillimanite: Mullite Compositions with Sillimanite-Type Superstructures," *Phys. Chem. Miner.*, **1**, 265–72 (1977).

[22]R. G. Burns, *Mineralogical Applications of Crystal Field Theory*, Ch. 4 and 5. Cambridge University Press, Cambridge, U.K., 1993.

[23]J. A. Tossel, D. J. Vaughan, and K. H. Johnson, "The Electronic Structure of Rutile, Wustite and Hematite from Molecular Orbital Calculations," *Am. Mineral.*, **59**, 319–34 (1974).

[24]N. Malengreau, J. P. Muller, and G. Calas, "Spectroscopic Approach for Investigating the Status and Mobility of Ti in Kaolinitic Materials," *Clays Clay Miner.*, **43** [5] 615–621 (1995).

[25]R. V. Morris and V. Lauer, "Matrix Effects for Reflectivity Spectra of Dispersed Nanophase (Superparamagnetic) Hematite with Application to Martian Spectral Data," *J. Geophys. Res.*, **95** [B4] 5101–109 (1990).

[26]H. Schneider, "Temperature-Dependent Iron Solubility in Mullite," *J. Am. Ceram. Soc.*, **70** [3] C-43–C-45 (1987).

[27]M. K. Murthy and F. A. Hummel, "X-ray Study of the Solid Solution of TiO_2, Fe_2O_3 and Cr_2O_3 in Mullite ($3Al_2O_3{\cdot}2SiO_2$)," *J. Am. Ceram Soc.*, **43**, 267–73 (1960). □